

## Supplemental Material for Temperature-sensitive colloidal phase behavior induced by critical Casimir forces

Minh Triet Dang,<sup>1</sup> Ana Vila Verde,<sup>2</sup> Van Duc Nguyen,<sup>1</sup> Peter G. Bolhuis,<sup>3</sup> and Peter Schall<sup>1</sup>

<sup>1</sup>*Van der Waals-Zeeman Institute, University of Amsterdam, Science Park 904, 1098 XH Amsterdam, The Netherlands*

<sup>2</sup>*Max Planck Institute of Colloids and Interfaces, Theory and Bio-Systems Department, Golm, Germany <sup>a)</sup>*

<sup>3</sup>*Van't Hoff Institute for Molecular Science, University of Amsterdam, Science Park 904, 1098 XH Amsterdam, The Netherlands*

(Dated: 21 June 2013)

---

<sup>a)</sup>Also at University of Minho, Physics Center, Campus de Gualtar, 4710-057 Braga, Portugal.

## I. SECOND VIRIAL COEFFICIENT FOR EVALUATING EXPERIMENTAL AND FITTED POTENTIALS

We calculate the normalized second virial coefficient,  $B_2^*$ , according to<sup>1</sup>:

$$B_2^* = -\frac{2\pi}{B_{2,HS}} \int_0^\infty r^2 [\exp(-\beta U(r)) - 1] dr. \quad (1)$$

In this expression,  $B_{2,HS} = 2/3\pi D^3$  is the second virial coefficient for a system of hard spheres of diameter  $D$ , and  $U(r)$  is the interparticle potential given in Fig. 1 of the main text. For  $0 < r \leq 1.11\sigma$  in system 1 and  $0 < r \leq 0.75\sigma$  in system 2 the potential is too repulsive to be accurately measured in experiment. To integrate equation 1 we thus used  $U(r) = \infty$  for  $0 < r \leq 1.11\sigma$  in system 1 and  $0 < r \leq 0.75\sigma$  in system 2. Integration is stopped at  $r = 3.6\sigma$  because all potentials are approximately zero at that interparticle separation. The hard sphere second virial coefficient used for normalization is that for hard spheres of diameter  $1.11\sigma$  (system 1) or  $0.75\sigma$  (system 2).

## II. GIBBS ENSEMBLE SIMULATIONS

Calculating the properties of coexisting gas and liquid phases from a simulation where both phases are in direct contact with each other requires a very large simulation box so that the fraction of particles at the gas-liquid interface is small and bulk (gas or liquid) properties can be calculated. This drawback is avoided in Gibbs ensemble<sup>2,3</sup> simulations by simulating each phase in a separate simulation box so that a physical gas-liquid interface does not exist. Coexistence is ensured by allowing the boxes to exchange particles and volume: the full system (box I + box II) is simulated in the NVT ensemble. As a result, the system spontaneously finds the coexistence gas and liquid densities for a given experimental temperature  $T$ . The full gas-liquid coexistence curve is obtained by performing simulations at closely spaced temperatures in the desired experimental temperature range. Using Gibbs ensemble simulations, bulk gas or liquid properties can be accurately calculated for all temperatures away from the colloidal critical point; when close to the critical point, transient interfaces between gas and liquid phases can form and this technique no longer yields reliable results.

For each  $\Delta T$ , we simulate a system of two cubic simulation boxes with a fixed number of 2000 colloidal particles in each box for system 1 and 1372 for system 2. The initial

configuration is obtained by first placing the particles in a face-centered cubic (FCC) lattice, and then running a preliminary simulation using a Casimir potential at  $\Delta T = -0.5^\circ\text{C}$  for system 1 and  $\Delta T = -0.3^\circ\text{C}$  for system 2. This procedure ensures that distinct gas and liquid equilibrium phases are present in the simulation boxes. Each simulation consists of at least  $5 \times 10^5$  (system 1) or  $2 \times 10^6$  (system 2) Monte Carlo (MC) cycles. Each simulation cycle contains three MC steps: a particle displacement step within one of the boxes, a change of the volume of the two boxes, and an exchange of particles between boxes. The magnitude of the Monte Carlo particle displacement and volume change is adjusted so that the acceptance ratio is 20%-50%.

At the end of each simulation, one box contains the vapor phase and the other the liquid phase. Far above the colloidal critical temperature, we obtain two narrow and clearly separated probability volume fraction peaks clearly pinpointing equilibrium gas and liquid densities, as illustrated in Fig. (1a) . Close to the colloidal critical point, the separation of peaks is no longer clearly distinct (Fig. 1b). Under these conditions, the free energy penalty for forming gas-liquid interfaces becomes very small<sup>4</sup>, so transient interfaces appear in both boxes. This appearance of transient interfaces increases the uncertainty associated with the volume fractions of the coexisting phases as is evident from the figure.

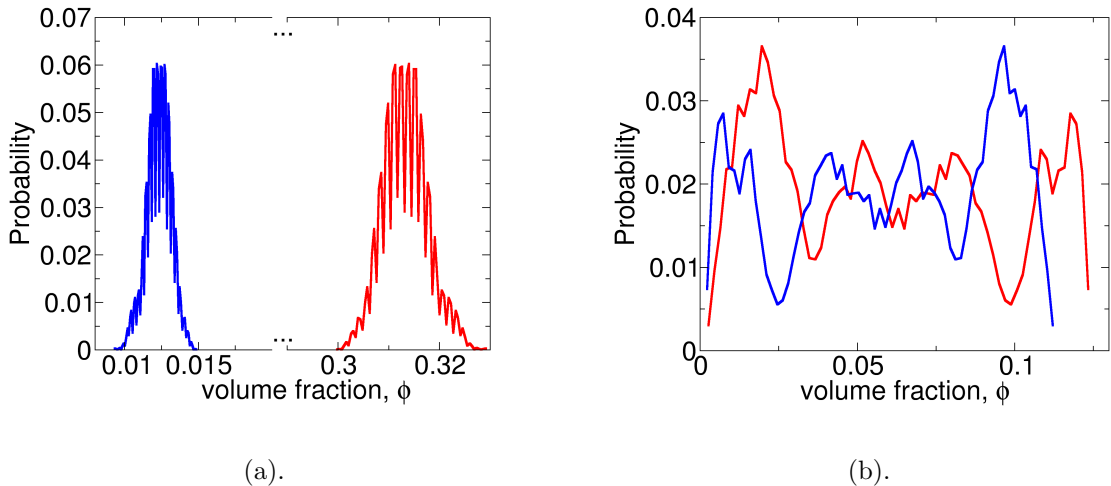


FIG. 1. Probability of each of the simulation boxes (red or blue) having  $\phi$  volume fraction of particles at  $\Delta T = -0.30^\circ\text{C}$  (a) and  $\Delta T = -0.32^\circ\text{C}$  (b) for system 2.

### III. GIBBS-DUHEM INTEGRATION

We use Gibbs-Duhem integration<sup>5</sup> to compute the full fluid-solid coexistence curve as a function of the experimental temperature  $T$ . In Gibbs-Duhem integration, the coexistence curve is obtained by numerically integrating the Gibbs-Duhem equation starting from a known reference coexistence point. For our system the relevant reference point is the hard sphere system coexistence<sup>6</sup> at a pressure of  $\beta P/\sigma^3 = 11.67$  and volume fractions  $\phi_l = 0.494$  and  $\phi_s = 0.545$ , for the liquid and the FCC crystal phases respectively. We perform the integration in two steps<sup>2</sup>. For clarity and convenience, we associate each integration step to one type of temperature: the simulation temperature  $T_\beta$  (first step) or the experimental temperature  $T$  (second step). The simulation temperature  $T_\beta$  is the reduced temperature in the simulation program. Unless otherwise noted, this temperature is kept constant at  $\beta = 1/(k_B T_\beta) = 1$ . The experimental temperature is the temperature at which the experiments were performed. Changes in this temperature are set in the simulations through changes in the input potential. We first integrate the regular Clausius-Clapeyron equation from the hard sphere reference system to the purely repulsive colloidal particles at  $\Delta T = -0.9^\circ\text{C}$  (system 1) and  $\Delta T = -0.7^\circ\text{C}$  (system 2), where critical Casimir forces are still negligible. This is done by adding a hard sphere potential to the repulsive potential  $\beta U_{cc} = \beta U_{rep}(r) + \beta U_{HS}(r)$ , where the hard sphere diameter is set to  $\sigma$ . For  $\beta = 0$  only the hard sphere potential remains, while at  $\beta = 1$  the full repulsive colloidal potential is recovered. The integration of the Clausius-Clapeyron equation for  $U_{rep}(r)$  along the coexistence line is performed using a predictor-corrector algorithm for a series of constant pressure MC simulations of both the FCC crystal and the liquid at different values of  $\beta$  with spacing of  $\Delta\beta = 0.1$  for both systems. In the second step we integrate from  $\Delta T = -0.9^\circ\text{C}$  (system 1) and  $\Delta T = -0.7^\circ\text{C}$  (system 2), and  $\beta = 1$  for both systems, to the desired final experimental temperature using the temperature-dependent total potential  $U(r; T)$ . Starting from the pressure  $\beta P/\sigma^3 = 55.76$  (system 1) and  $\beta P/\sigma^3 = 20.08$  (system 2) and the solid and liquid volume fractions for  $\beta = 1$  obtained in the first step, we integrate  $\frac{dP}{dT} = -\Delta(\frac{\partial g}{\partial T})/\Delta v = -\langle\frac{du}{dT}\rangle/\Delta v$ , where  $\Delta$  indicates the difference between the solid and liquid phase,  $v$  is the molar volume,  $g$  the molar Gibbs free energy, and  $u$  the molar potential energy. The angular brackets denote an ensemble average. Again, the integration is performed using a predictor-corrector algorithm for a series of constant pressure MC simu-

lations of both the solid and the liquid for different experimental temperatures  $T$ . In what follows we describe the Gibbs-Duhem equations that apply to each integration step.

Consider a system of  $N$  monodisperse colloids whose position vectors are denoted by  $(r_1, \dots, r_N) \equiv r^N$ . The pair interaction potential between these particles is  $U = U(r; T)$ . The Gibbs free energy  $G$  and the chemical potential describing the thermodynamic properties of this system are  $G(N, P, T_\beta, T) = N\mu(P, T_\beta, T)$ , where  $P$  is the pressure.

In the isobaric-isothermal ensemble, the Gibbs free energy can be obtained from the partition function by the relation

$$\beta G(N, P, T_\beta, T) = -\ln Q_{NPT_\beta}(T), \quad (2)$$

and

$$Q_{NPT_\beta}(T) \propto \int dV e^{-\beta PV} \int_V dr^N e^{-\beta U(r^N, T)}, \quad (3)$$

where  $V$  is the volume of the  $N$  particles.

Consider also that this system is initially in an equilibrium state characterized by two coexisting phases (solid and liquid). Each of the phases can be considered a thermodynamic system of their own, characterized by the Gibbs-Duhem equation of the form:

$$d\mu = -s dT_\beta + v dP + \frac{\partial g}{\partial T} dT, \quad (4)$$

where  $s = S/N$ ,  $g = G/N$ ,  $v = V/N$ , respectively, are the molar entropy, molar Gibbs free energy and molar volume. If the system is reversibly perturbed (by  $dT$ ,  $dT_\beta$  and  $dP$ ), it will reach a new equilibrium state. During this process, the two coexisting phases (labeled as *liq*, *sol*) remain in equilibrium, so the change in their chemical potential  $\mu$  must satisfy:

$$d\mu_{sol} = d\mu_{liq}. \quad (5)$$

Thus, the chemical potential difference between the two phases can be written as:

$$d\mu_{sol} - d\mu_{liq} = -(s_{sol} - s_{liq})dT_\beta + (v_{sol} - v_{liq})dP + \left( \frac{\partial g_{sol}}{\partial T} - \frac{\partial g_{liq}}{\partial T} \right) dT = 0. \quad (6)$$

The liquid-solid coexistence curve is determined by integrating equation 6. As mentioned above, for convenience this integration is done in two integration steps.

*Integration step 1:* At constant experimental temperature  $T$ , eq. 6 reduces to the Clausius Clapeyron equation:

$$\frac{dP}{dT_\beta} = \frac{s_{sol} - s_{liq}}{v_{sol} - v_{liq}} = \frac{\Delta s}{\Delta v}. \quad (7)$$

It is convenient to formulate eq. 7 in a form that can more easily be integrated in simulation. We first re-write it as a differential of  $\beta P$  with respect to  $\beta$ :

$$\frac{d\beta P}{d\beta} = -\frac{1}{\beta} \frac{\Delta s}{\Delta v} + P. \quad (8)$$

As at coexistence the pressure, temperature and chemical potential of the two phases are identical, the change in entropy can be expressed as a function of the molar potential energy  $u$  and enthalpy  $h$ :

$$T_\beta \Delta s = \Delta h = \Delta u + P \Delta v. \quad (9)$$

The final form of the Clausius Clapeyron equation directly follows from substituting eq. 7 in eq. 9:

$$\frac{d\beta P}{d\beta} = -\frac{\Delta u}{\Delta v}. \quad (10)$$

*Integration step 2:* At  $\beta = 1$  in equilibrium, the pressure change with respect to the change of experimental temperature  $T$  can be written as:

$$\frac{dP}{dT} = -\frac{1}{v_{sol} - v_{liq}} \left( \frac{\partial g_{sol}}{\partial T} - \frac{\partial g_{liq}}{\partial T} \right) = -\Delta \left( \frac{\partial g}{\partial T} \right) / \Delta v = -\left\langle \frac{du}{dT} \right\rangle / \Delta v. \quad (11)$$

The last equality follows from an explicit expression of the derivative of the molar Gibbs free energy  $g(T)$  with respect to  $T$  as:

$$\begin{aligned} \frac{\partial g}{\partial T} &= -\frac{1}{\beta} \frac{\partial}{\partial T} \ln Q_{NPT_\beta} = -\frac{1}{\beta Q_{NPT_\beta}} \frac{\partial Q_{NPT_\beta}}{\partial T} \\ &= \frac{\int dV e^{-\beta PV} \int dr^N \left( \frac{\partial u}{\partial T} \right) e^{-\beta u}}{\int dV e^{-\beta PV} \int dr^N e^{-\beta u}} \\ &= \left\langle \frac{\partial u}{\partial T} \right\rangle, \end{aligned} \quad (12)$$

where the brackets denote an average over the isothermal-isobaric  $NPT_\beta$  ensemble. Using the fact that the energy is a sum of pair potentials we can write the last average as

$$\left\langle \frac{\partial u}{\partial T} \right\rangle = \left\langle \sum_{i<j} \frac{\partial U(r_{ij}, T)}{\partial T} \right\rangle. \quad (13)$$

For each integration step we perform Monte Carlo simulations of a system with two cubic boxes, one for each phase. Simulations are performed in the isothermal-isobaric  $NPT_\beta$  ensemble with 2084 particles in each box for system 1 and 864 for system 2. The initial conditions for simulations of each state point are obtained from the final configurations (pressure, volume fraction and particle coordinates of each phase) of the preceding run. We

use periodic boundary conditions and a cutoff distance of  $r_c = 4.5\sigma$  for system 1 and  $3.5\sigma$  for system 2. Each simulation is equilibrated for  $5 \times 10^3$  (system 1) or  $6.25 \times 10^4$  (system 2) MC cycles; production runs are of the same length as equilibration. One MC cycle consists of an attempt to displace all particles in the system and one attempted volume change. The magnitude of the Monte Carlo moves is adjusted so that the acceptance ratio is 40%-50%.

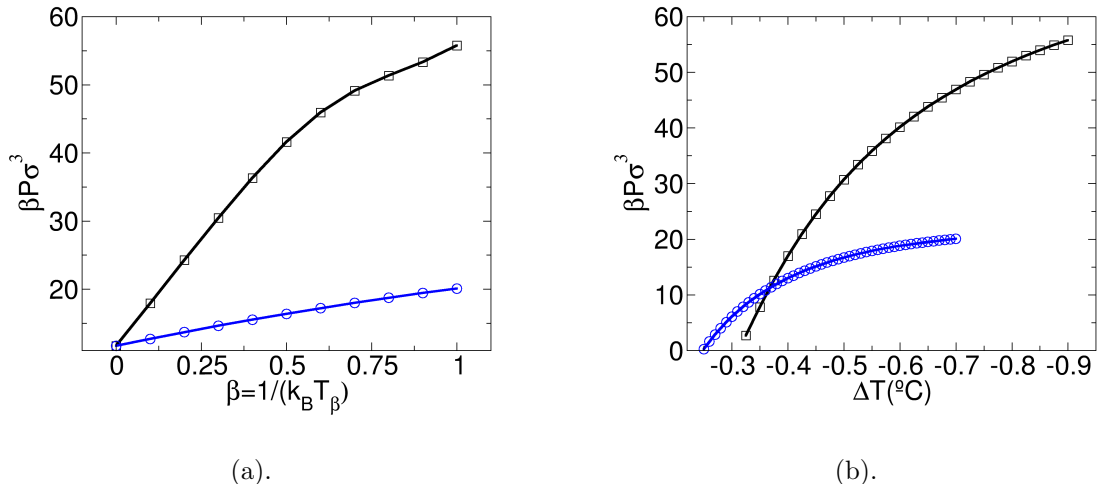


FIG. 2. Gibbs-Duhem integration: Solid-fluid coexistence pressure vs. reciprocal temperature (a) and experimental temperature (b) for system 1 (black) and system 2 (blue).  $\beta P \sigma^3$  is the reduced pressure ( $\beta$  and  $\sigma$  are unity). Solid lines are guides to the eye.

The first Gibbs-Duhem integration step results in a rapid increase of pressure with increasing reciprocal temperature, as shown in Fig. 2a. This increase in pressure reflects the increasingly longer-range repulsive interaction between the colloids.

The second step results in an decrease of pressure as  $\Delta T$  becomes less negative, i.e. with increasing experimental temperature  $T$ , as shown in Fig. 2b. Starting from a high pressure at low temperature, the pressure decreases with increasing temperature, as attraction between particles becomes stronger.

#### IV. SCALING

As described in the main text, the scaling relations<sup>2</sup>

$$\frac{\phi_l + \phi_g}{2} = \phi_C + A(T - T_C) \quad (14)$$

and

$$\phi_l - \phi_g = B(T - T_C)^{\beta_c} \quad (15)$$

with  $\beta_c = 0.325$  were used to estimate the critical temperature  $\Delta T_C$  and volume fraction  $\phi_C$  for each system by fits to the calculated gas-liquid coexistence curves. The critical constants and the fitting parameters  $A$  and  $B$  obtained from these fits are shown in Table I.

TABLE I. Critical temperature  $\Delta T_C$ , critical volume fraction  $\phi_C$ , and fitting parameters  $A$  and  $B$  obtained from fitting Eqs. 14 and 15 to the gas-liquid coexistence curves of each system.

	System 1	System 2
$A$	1.0046	1.3125
$B$	0.8852	1.067
$\Delta T_C$ (°C)	-0.38	-0.32
$\phi_C$	0.115	0.134

Re-writing eqs. 14 and 15 in terms of temperature differences,  $\Delta T = T - T_{cx}$  and  $\Delta T_C = T_C - T_{cx}$ , we obtain

$$\frac{\phi_g}{\phi_C} = 1 - \frac{A\Delta T_C}{\phi_C} \left(1 - \frac{\Delta T}{\Delta T_C}\right) - \frac{B|\Delta T_C|^{\beta_c}}{2\phi_C} \left(1 - \frac{\Delta T}{\Delta T_C}\right)^{\beta_c} \quad (16)$$

$$\frac{\phi_l}{\phi_C} = 1 - \frac{A\Delta T_C}{\phi_C} \left(1 - \frac{\Delta T}{\Delta T_C}\right) + \frac{B|\Delta T_C|^{\beta_c}}{2\phi_C} \left(1 - \frac{\Delta T}{\Delta T_C}\right)^{\beta_c} \quad (17)$$

As shown in the main text, equations 16 and 17 together with the parameters in Table I describe the scaled gas-liquid coexistence curve well.

## REFERENCES

- <sup>1</sup>M. E. Tuckerman, *Statistical mechanics: theory and molecular simulation* (Oxford university press, 2011).
- <sup>2</sup>D. Frenkel and B. Smit, *Understanding Molecular Simulation, Second Edition: From Algorithms to Applications* (Academic Press, San Diego, California, USA, 2001).
- <sup>3</sup>A. Z. Panagiotopoulos, *Mol. Phys.* **61**, 813 (1987).
- <sup>4</sup>B. Smit, P. Desmedt, and D. Frenkel, *Mol. Phys.* **68**, 931 (1989).
- <sup>5</sup>D. A. Kofke, *J. Chem. Phys.* **98**, 4149 (1993).
- <sup>6</sup>W. Hoover and F. Ree, *J. Chem. Phys.* **49**, 3609 (1968).